

## Anomalous Pseudogap Formation in a Nonsuperconducting Crystal of $\text{Nd}_{1.85}\text{Ce}_{0.15}\text{CuO}_{4+y}$ : Implication of Charge Ordering

Y. Onose, Y. Taguchi, T. Ishikawa, S. Shinomori, K. Ishizaka, and Y. Tokura

*Department of Applied Physics, University of Tokyo, Tokyo 113-8656, Japan*

(Received 4 November 1998; revised manuscript received 26 January 1999)

Temperature variation of optical conductivity and Raman spectra has been investigated comparatively for oxygenated antiferromagnetic and reduced superconducting crystals of  $\text{Nd}_{1.85}\text{Ce}_{0.15}\text{CuO}_{4+y}$ . While the spectra of the reduced crystal change little with temperature, in the spectra of oxygenated crystal a conspicuous pseudogap structure evolves around 0.3 eV and activated infrared and Raman Cu-O phonon modes grow in intensity, with decreasing temperature from 340 K. The origin is proposed to be charge ordering instability induced by a minute amount of interstitial apical oxygen, which seems to be also responsible for the absence of superconductivity in an oxygenated (or as-grown) crystal. [S0031-9007(99)09444-2]

PACS numbers: 74.72.Jt, 71.45.Lr, 75.50.Ee, 78.30.-j

Although most high- $T_c$  cuprate superconductors are obtained by doping holes into antiferromagnetic insulators, there is a class of materials,  $\text{Ln}_{2-x}\text{Ce}_x\text{CuO}_4$  ( $\text{Ln} = \text{Nd, Pr, Sm, and Eu}$ ), with so-called  $T'$  structure, in which the  $\text{CuO}_2$  planes can be doped with electrons [1,2]. A long-standing mystery for the  $T'$ -structure superconductors is the effect of an oxygen-reducing procedure. Superconductivity shows up only when samples with a narrow range of Ce concentration ( $0.14 < x < 0.17$ ) are subject to an appropriate reducing procedure but never manifests itself in any Ce concentration in as-grown or oxygenated crystals [2]. In the as-grown or oxygenated compounds with  $x = 0.15$ , antiferromagnetic long-range order is observed to set in at  $T_N = 120\text{--}160$  K [3–5]. The reducing procedure and resultant removal of oxygen might increase the electron-doping level. However, there should be a more important role of the reducing procedure in inducing superconductivity, since superconductivity is not observed for the crystals without reducing procedure even when the doping level is higher than 0.15. A recent neutron diffraction experiment on a single crystal has revealed [6] that a minute amount ( $\Delta y \approx 0.02$ ) of interstitial apical oxygens in  $\text{Nd}_{2-x}\text{Ce}_x\text{CuO}_{4+y}$ , which should be absent in the ideal  $T'$  structure, are removed by the reducing procedure. Therefore, the presence of apical oxygens as “impurities” seems to be decisive of the ambivalence between the two phases, superconductivity vs antiferromagnetism. Such impurities may lead to a local lattice distortion as observed by neutron diffraction experiment with a pair distribution function analysis [7] and Raman scattering [8] and thus significantly modify the electronic structure in the  $\text{CuO}_2$  plane. In order to elucidate the hidden role of the apical oxygen, we have investigated temperature variation of optical spectra comparatively for both oxygenated and reduced single crystals of  $\text{Nd}_{1.85}\text{Ce}_{0.15}\text{CuO}_{4+y}$ . Only for the oxygenated crystal, we have found anomalous pseudogap formation accompanied by lowering of the local lattice symmetry, which is reminiscent of a typical charge ordering transition [9–11].

Single crystals of  $\text{Nd}_{1.85}\text{Ce}_{0.15}\text{CuO}_{4+y}$  were grown by the traveling solvent floating-zone method in  $\text{O}_2$  atmosphere of 4 atm. The  $c$ -axis lattice constant agrees well with the previously reported value [2], which indicates that the Ce concentration coincides with the prescribed value ( $x = 0.15$ ). To obtain superconducting samples, some pieces from a crystal boule were annealed in flowing Ar gas for 100 hours at  $1000^\circ\text{C}$  and subsequently in  $\text{O}_2$  for 50 hours at  $500^\circ\text{C}$ . As reported repeatedly in literature [6], the reduction ( $\Delta y$ ) in oxygen content in  $\text{Nd}_{2-x}\text{Ce}_x\text{CuO}_{4+y}$  is merely  $< 0.02$  by such a reducing procedure, yet the superconductivity emerges with full phase volume. Both resistivity and susceptibility measurements showed an onset of superconducting transition at 25 K and the shielding fraction reaches almost 100% already at 20 K for the reduced crystal. Reflectivity and Raman spectra were measured on the  $ab$  face of the nonsuperconducting and superconducting crystals with the typical size of  $6 \times 4 \times 2$  mm<sup>3</sup>. The  $ab$  face was polished with alumina powder to a mirrorlike surface. To remove possible stress at the polished surface, we annealed the as-grown crystal in  $\text{O}_2$  for 100 hours at  $1000^\circ\text{C}$  and the reduced crystal at  $500^\circ\text{C}$  in Ar for 50 hours after polishing.

In measurements of reflectivity spectra, we used Fourier spectroscopy for a photon energy range of 0.01–0.8 eV and grating spectroscopy for 0.6–36 eV. For a high-energy region ( $> 6$  eV), the reflectivity spectra were measured with the use of synchrotron radiation at INS-SOR, Institute for Solid State Physics, University of Tokyo. Temperature dependence of the reflectivity spectra was measured for 0.01–3 eV over the range of 10–390 K. The room temperature data for above 3 eV were used to perform the Kramers-Krönig analysis and deduce optical-conductivity spectra at respective temperatures. For the analysis, we assumed constant reflectivity or the Hagen-Rubens relation below 0.01 eV and  $\omega^{-4}$  extrapolation above 36 eV. Raman scattering spectra were measured with the use of a 514.5 nm line from an argon ion laser as an incident light. The backward

scattered light was collected and dispersed by a triple monochromator equipped with a liquid-nitrogen-cooled charge-coupled device detector.

We show in the inset in Fig. 1 temperature dependence of resistivity for both the oxygenated and the reduced crystals. With lowering temperature, the resistivity shows a gradual upturn at around 200 K for the oxygenated crystal, while the reduced crystal shows a superconducting transition at 25 K. Note that resistivity for the oxygenated crystal is fairly low ( $\rho \sim 2 \text{ m}\Omega \text{ cm}$ ) even at the lowest temperature (4.2 K), indicating a still itinerant nature of charge carriers in the antiferromagnetic phase. Resistivity of the reduced crystal at 25 K (immediately above  $T_c$ ) is  $28 \mu\Omega \text{ cm}$ , the lowest value ever reported for the samples with the same doping level, signaling the high quality of the present crystal.

Reflectivity spectra of the oxygenated and reduced crystals at 10 and 290 K are shown in Fig. 1. Spectra in a lower energy region below 3 eV are all related to antibonding states composed of O  $2p$  and Cu  $3d_{x^2-y^2}$  orbitals besides optical phonon excitations [13]. In the spectrum of the oxygenated crystal, a broad peak is discernible at around 2 eV and is ascribed to the remnant of charge-transfer gap excitation from O- $2p$ -like states to Cu- $3d$ -like states. Below 1 eV, a high-reflectance metallic band arises but the optical phonon modes are clearly discerned in a far-infrared region ( $\hbar\omega < 0.07 \text{ eV}$ ), indicating a poor dielectric screening effect. In the spectrum at 10 K, there is a hollow structure in a mid-infrared region ( $\hbar\omega = 0.2\text{--}0.3 \text{ eV}$ ) and also a broad peak structure at around 0.05 eV, both of which are hardly discernible in the spectrum at 290 K. These structures are responsible for a gaplike structure (0.2–0.3 eV) and activated phonon structure (around 0.042 eV), respectively, in the optical conductivity spectrum (see Figs. 2 and 3). Upon the reducing procedure, the reflectivity below 1 eV is increased, and the two structures observed in the oxygenated crystal become indiscernible at 10 K as well as at 290 K.

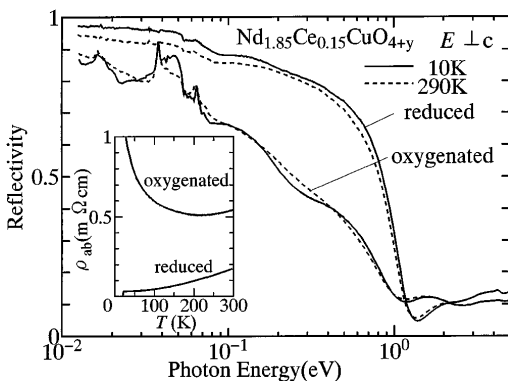


FIG. 1. Reflectivity spectra for an oxygenated (nonsuperconducting) and a reduced (25 K superconducting) crystal of  $\text{Nd}_{1.85}\text{Ce}_{0.15}\text{CuO}_{4+y}$  at 10 and 290 K. The inset shows the temperature dependence of in-plane resistivity for the both crystals.

We show in Fig. 2(a) optical conductivity spectra of the oxygenated and reduced crystals at 10 and 290 K, derived from the reflectivity spectrum by the aforementioned Kramers-Krönig analysis. At 290 K, the spectrum for the oxygenated crystal shows a broad incoherent mid-infrared absorption, which reproduces the feature reported by previous studies [12,13] and is also common to those seen in the hole-doped systems [14,15]. When the temperature is lowered down to 10 K, the spectral weight is transferred from the region of 0.1–0.3 eV to a higher energy region, forming a gaplike structure. Note that temperature variation in the spectrum for the oxygenated crystal extends up to 1 eV or higher. In the reduced crystal, on the other hand, the shape of the low energy spectrum is more Drude-like. The reduced crystal shows little change in the spectrum (at least above 0.1 eV) when cooled down to 10 K. The pseudogap structure that is present in the oxygenated crystal is completely missing in the reduced sample. The observed difference of the 290 K optical conductivity spectra for the oxygenated and reduced crystals is due partly to the reducing-induced increase of electron-type carriers, as previously demonstrated by the optical study on  $\text{Pr}_{2-x}\text{Ce}_x\text{CuO}_4$  crystals with and without the reducing procedure [13]. Judging from a large-energy scale change of the spectrum with temperature, however, we should consider that interstitial apical oxygen plays another important role in essential modification of electronic structure. One might argue that random distribution of apical oxygen in oxygenated crystal and resultant Anderson localization of charge carriers are responsible

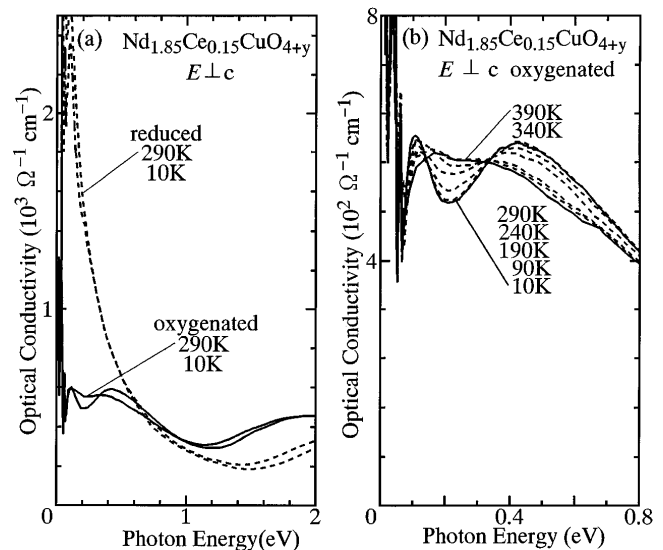


FIG. 2. (a) Optical conductivity spectra for an oxygenated crystal (solid line) and a reduced crystal (dashed line) of  $\text{Nd}_{1.85}\text{Ce}_{0.15}\text{CuO}_{4+y}$  at 10 and 290 K. (b) Temperature dependence of optical conductivity spectra for an oxygenated crystal of  $\text{Nd}_{1.85}\text{Ce}_{0.15}\text{CuO}_{4+y}$  in a mid-infrared region, showing the pseudogap feature.

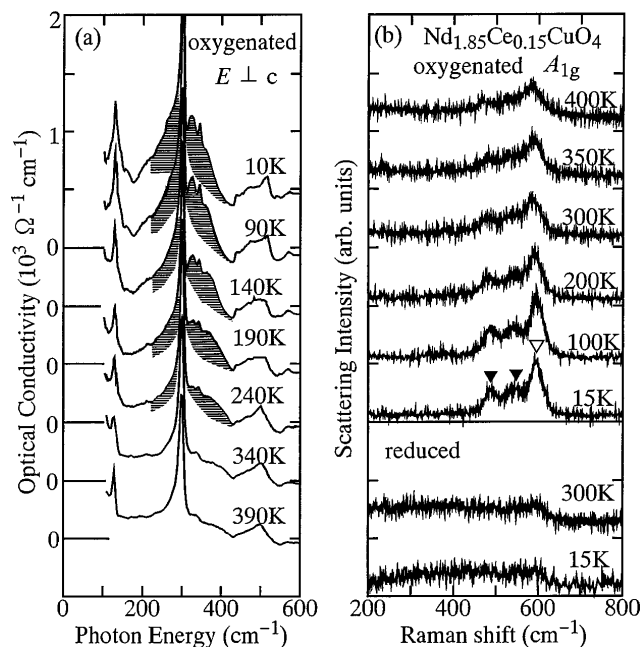


FIG. 3. (a) Temperature dependence of optical conductivity spectra for an oxygenated crystal of  $\text{Nd}_{1.85}\text{Ce}_{0.15}\text{CuO}_{4+y}$  in a low energy region below  $600\text{ cm}^{-1}$ , showing the phonon anomaly (mainly a hatched region). (b) Temperature dependence of  $A_{1g}$  Raman spectra for an oxygenated and a reduced crystal of  $\text{Nd}_{1.85}\text{Ce}_{0.15}\text{CuO}_{4+y}$ . In addition to the imperfection-induced mode (an open triangle) at  $600\text{ cm}^{-1}$ , closed triangles indicate the activated modes by lowering temperature.

for the pseudogap formation. However, an energy scale of  $1\text{ eV}$  observed for the spectral change can not be accounted for in terms of localization phenomena, whose energy scale must be by 2 orders of magnitude smaller.

We show in Fig. 2(b) temperature dependence of the optical conductivity for the oxygenated crystal in more detail. As shown in Fig. 2(b), spectral weight between  $0.1$  and  $0.3\text{ eV}$  is gradually transferred across the isobetic (equal absorption) point at  $0.3\text{ eV}$  to a higher energy region ( $\geq 0.3\text{ eV}$ ) with decreasing temperature below  $340\text{ K}$ . Since the spectral shape shows no more temperature-dependence above  $340\text{ K}$ , it is likely that the pseudogap formation sets in at around this temperature. Evolution of the pseudogap structure at low temperatures is nearly saturated below  $90\text{ K}$ , although complete opening of a gap (i.e., zero conductivity in  $\omega \rightarrow 0$ ) is not achieved even at the lowest temperature.

We show in Fig. 3(a) the temperature variation of the optical conductivity spectra below  $600\text{ cm}^{-1}$ . If the crystal were ideally tetragonal, four phonon modes would be expected for in-plane polarization from the factor group analysis. Four phonon modes are actually observed, e.g., around  $0.016$ ,  $0.037$ ,  $0.042$ , and  $0.063\text{ eV}$  ( $130$ ,  $300$ ,  $340$ , and  $510\text{ cm}^{-1}$ ) in the conductivity spectra above  $340\text{ K}$ . The assignment of the optical phonon modes at  $0.035$ – $0.045\text{ eV}$  ( $280$ – $360\text{ cm}^{-1}$ ) has not reached a consensus in literature [16,17]. In contrast to a relatively narrow

$0.037\text{ eV}$  ( $300\text{ cm}^{-1}$ ) peak, three other modes are rather broad in width and show asymmetric shape, indicating strong coupling with the electronic background. This narrow  $0.037\text{ eV}$  mode is hence assigned here to oxygen vibration in the  $(\text{Nd,Ce})_2\text{O}_2$  layer, which is consistent with Tajima *et al.* [17]. The broad band centered around  $0.042\text{ eV}$  ( $340\text{ cm}^{-1}$ ) [hatched structure in Fig. 3(a)] grows in intensity with decreasing temperature from  $340\text{ K}$  in this region, where some sharp modes are buried in, or interfere with, this broad band. In particular, Fano resonance phonon structures can be clearly discerned on the higher energy side of the  $0.037\text{ eV}$  sharp phonon mode at least below  $190\text{ K}$ . We assigned the broad band mode to the Cu-O bending mode activated by lowering symmetry and hybridization with electronic background. Importantly, this broad Cu-O bending mode is nearly absent above  $340\text{ K}$  and remarkably grows in intensity with decreasing temperature from  $340\text{ K}$ , signaling a change in the electronic system.

To discuss a more quantitative aspect, we plot in Fig. 4 as a function of temperature the change in spectral weight between  $0.145$  and  $0.33\text{ eV}$ , and between  $0.030$  and  $0.046\text{ eV}$  ( $240$  and  $370\text{ cm}^{-1}$ ) as measures of electronic pseudogap and lattice distortion, respectively. These quantities in units of effective number of electrons ( $N_{\text{eff}}$ ) are estimated as the difference from those at  $390\text{ K}$ , where conductivity spectrum shows no more temperature variation. These quantities vary with temperature in an almost parallel manner below  $390\text{ K}$ . It is clear from Fig. 4 that the pseudogap formation with lattice distortion begins at about  $340\text{ K}$ , which is much higher than the antiferromagnetic transition ( $120$ – $160\text{ K}$  [4,5]) and the resistivity upturn (around  $200\text{ K}$ ).

The anomaly of lattice dynamics in lowering temperature is also seen in Raman spectra. We exemplify in Fig. 3(b) the temperature variation of Raman spectra of the  $A_{1g}$  symmetry. Some activated phonon peaks show up around  $600\text{ cm}^{-1}$  for the oxygenated (nonsuperconducting) crystal, as also reported in literature [18], while no more modes are discernible for the reduced (superconducting) crystal. These activated phonon modes, in particular, for the main peak at  $600\text{ cm}^{-1}$ , may arise from the local lattice distortion (perhaps due to the presence of apical oxygen in oxygenated crystal [8]) and subsist even above  $400\text{ K}$ . Note, however, that new modes [indicated by closed triangles in Fig. 3(b)] are remarkably activated at the lower energy side of the  $600\text{ cm}^{-1}$  main peak (an open triangle) with decreasing temperature and that the total intensity of these modes increases in accord with the evolution of pseudogap formation and infrared Cu-O phonon anomaly. Thus, the Raman spectra of the oxygenated crystal provide another evidence for the lattice anomaly coupled with a change of electronic structure.

One might think that the pseudogap formation stems from a conventional spin-density wave (SDW) transition in a low dimensional system, but this possibility is

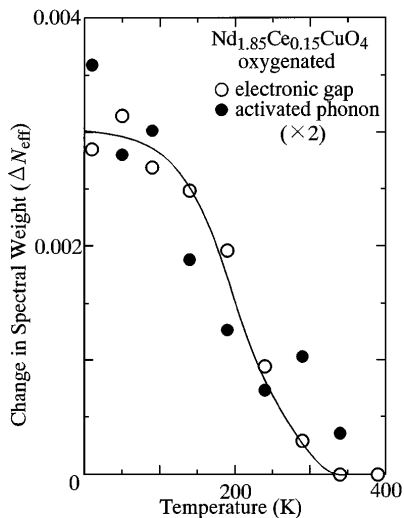


FIG. 4. Temperature variation of spectral weight in the region of 0.145–0.330 eV (open circles) due to electronic pseudogap formation, and in the region of 0.030–0.046 eV (closed circles) due to the activated phonon modes. These are plotted in units of effective number of electrons ( $N_{\text{eff}}$ ) and are defined as the difference from those at 390 K (see text). Solid line is a guide to the eyes.

definitely ruled out in the present case. The energy scale of the pseudogap ( $\sim 0.3$  eV) is too large to be assigned to the SDW-induced gap. The weak coupling theory [19] for the SDW transition predicts the value of  $2\Delta/k_B T_N = 3.5$ ,  $\Delta$  being the SDW gap and  $T_N$  being Néel temperature. In the present case,  $2\Delta$  of 0.3 eV and  $T_N \sim 150$  K yield the value of  $2\Delta/k_B T_N \sim 23$ , which is much larger than the theoretically predicted value and also than the experimentally observed values for canonical SDW transition systems, such as Cr ( $2\Delta/k_B T_N \approx 5.1$ ) [20] and (TMTSF) $_2$ PF $_6$  ( $2\Delta/k_B T_N \approx 8.4$ ) [21]. In addition, a possible nesting vector, which is expected from the band structure based on calculation [22] and angle resolved photoemission experiments [23,24], is along  $(\pi, 0)$ , but the actual Bragg spot observed in neutron diffraction [5] is around  $(\pi, \pi)$  in contradiction to such a simple expectation. Alternatively, we propose here that the anomalous pseudogap formation originates from charge ordering or its fluctuation which is induced by a minute amount of apical oxygen. In typical charge-ordering systems, such as La $_{1.67}$ Sr $_{0.33}$ NiO $_4$  [9], La $_{1/3}$ Sr $_{2/3}$ FeO $_3$  [10], and Pr $_{0.6}$ Ca $_{0.4}$ MnO $_3$  [11], commonly observed is spectral weight transfer over a wide energy region up to eV order, and concomitant anomalies in phonon modes. These features are quite parallel with what we have revealed for the oxygenated crystal of Nd $_{1.85}$ Ce $_{0.15}$ CuO $_{4+y}$ , although the pseudogap feature in this compound is contrasted with the real gap (i.e., total disappearance of the spectral weight at  $\hbar\omega = 0$ ) observed for the aforementioned systems. Recently, evidences have been accumulated for static stripe ordering in (La,Nd) $_{2-x}$ Sr $_x$ CuO $_4$  ( $x = 0.12$ ) [25]. In the case of Nd $_{1.85}$ Ce $_{0.15}$ CuO $_{4+y}$ , it is likely that a tiny amount

of apical oxygen act as impurities and induce charge ordering instability around them. The highly mobile character of charge carriers in this system may melt static ordering, or otherwise the inhomogeneity of apical oxygen location may produce the microscopic phase segregation into the charge-ordered and metallic phases, which results in the appearance of the pseudogap instead of the real gap.

In summary, temperature variation of optical spectra has been investigated for an oxygenated antiferromagnetic and a reduced superconducting crystal of Nd $_{1.85}$ Ce $_{0.15}$ CuO $_{4+y}$ . Only for the oxygenated crystal, a conspicuous pseudogap feature at around 0.3 eV as well as a local symmetry-lowering distortion was revealed in the optical spectra, which grows with lowering temperature below about 340 K in quite a parallel manner. We propose that these anomalies originate from charge ordering or its fluctuation induced by a minute amount of apical oxygens and that the superconductivity is completely extinguished by such a charge ordering fluctuation in this electron-doped cuprate without reducing procedure.

We thank Dr. T. Kimura for his helpful advice on crystal growth. This work was supported in part by Grant-in-Aids for Scientific Research from the Ministry of Education, Science, Sports, and Culture, Japan, and the New Energy and Industrial Technology Development Organization of Japan (NEDO).

- [1] Y. Tokura *et al.*, Nature (London) **337**, 345 (1989).
- [2] H. Takagi *et al.*, Phys. Rev. Lett. **62**, 1197 (1989).
- [3] G. M. Luke *et al.*, Nature (London) **338**, 49 (1989).
- [4] S. Kambe *et al.*, J. Phys. Soc. Jpn. **60**, 400 (1991).
- [5] M. Matsuda *et al.*, Phys. Rev. B **45**, 12 548 (1992).
- [6] A. J. Schultz *et al.*, Phys. Rev. B **53**, 5157 (1996).
- [7] S. J. L. Billinge *et al.*, Phys. Rev. B **47**, 14 386 (1993).
- [8] E. T. Heyen *et al.*, Phys. Rev. B **43**, 2857 (1991).
- [9] T. Katsufuji *et al.*, Phys. Rev. B **54**, R14 230 (1996).
- [10] T. Ishikawa *et al.*, Phys. Rev. B **58**, R13 326 (1998).
- [11] Y. Okimoto *et al.*, Phys. Rev. B **57**, R9377 (1998).
- [12] S. L. Cooper *et al.*, Phys. Rev. B **41**, 11 605 (1990).
- [13] T. Arima *et al.*, Phys. Rev. B **48**, 6597 (1993).
- [14] S. Uchida *et al.*, Phys. Rev. B **43**, 7942 (1991).
- [15] D. B. Romero *et al.*, Solid State Commun. **82**, 183 (1992).
- [16] E. T. Heyen *et al.*, Solid State Commun. **74**, 1299 (1990).
- [17] S. Tajima *et al.*, Phys. Rev. B **43**, 10 496 (1991).
- [18] V. G. Hadjiev *et al.*, Solid State Commun. **71**, 1093 (1989).
- [19] For example, G. Grüner, *Density Wave in Solids* (Addison-Wesley, Reading, MA, 1994).
- [20] A. S. Barker *et al.*, Phys. Rev. Lett. **20**, 384 (1968).
- [21] L. Degiorgi *et al.*, Phys. Rev. Lett. **76**, 3838 (1996).
- [22] S. Massidda *et al.*, Physica (Amsterdam) **157C**, 157 (1989).
- [23] D. M. King *et al.*, Phys. Rev. Lett. **70**, 3159 (1993).
- [24] R. O. Anderson *et al.*, Phys. Rev. Lett. **70**, 3163 (1993).
- [25] J. M. Tranquada *et al.*, Nature (London) **375**, 561 (1995); M. V. Zimmermann *et al.*, Europhys. Lett. **41**, 629 (1998); B. G. Levi, Phys. Today **51**, No. 6, 19 (1998).